Available online at www.sciencedirect.com
ScienceDirect
Journal of Magnetic Resonance 185 (2007) 247–258
JMR Journal of Magnetic Resonance
www.elsevier.com/locate/jmr

Theoretical studies of the effect of the dipolar field in multiple spin-echo sequences with refocusing pulses of finite duration

Chung Ki Wong [a], Scott D. Kennedy [b], Edmund Kwok [c], Jianhui Zhong [a,c,d,*]

[a] Department of Physics and Astronomy, University of Rochester, NY 14627, USA
[b] Department of Biochemistry and Biophysics, University of Rochester, NY 14627, USA
[c] Department of Radiology, University of Rochester, NY 14627, USA
[d] Department of Biomedical Engineering, University of Rochester, NY 14627, USA

Received 14 July 2006; revised 4 December 2006
Available online 10 January 2007

Abstract

It has been observed recently that the finite duration of refocusing rf pulses in a multiecho acquisition of the signal formed under the influence of the dipolar field leads to significant signal attenuation [S. Kennedy, Z. Chen, C.K. Wong, E.W.-C. Kwok, J. Zhong, Investigation of multiple-echo spin-echo signal acquisition under distant dipole–dipole interactions, Proc. Int. Soc. Magn. Reson. Med. 13 (2005) 2288]. Hereto, we quantify the phenomenon by evaluating analytically the influences of both the distant dipolar field (DDF) and transverse relaxation T_2 on the magnetization in a multiecho pulse sequence based on correlation spectroscopy revamped by asymmetric z-gradient echo detection (CRAZED). Analytic expressions for the magnetization were obtained, which demonstrate explicitly the origin of rephased signal in the presence of the finite π pulses in the multiecho train. The expressions also explain the effects of the DDF and T_2 during the refocusing pulses on the signal strength, and show the substantial signal dependence on the phase of the rf pulses. We show that when the DDF effect during the pulse is canceled, the signal rises primarily during the free evolution time in the acquisition period. This elucidates the signal attenuation when the rf pulses cover a significant proportion of time in the sequence. In addition, we performed an optimization on the number of refocusing pulses that maximizes the total acquired signal using parameters for water, brain white matter, and muscle. We found that maximal signal-to-noise ratio is obtained when the pulse duration approximately equals the free evolution time in the samples with a wide range of T_2.

Keywords: Distant dipolar field; Multiple spin-echo sequence; Finite pulse; Intermolecular double-quantum coherence

1. Introduction

It was noted in the early days of nuclear magnetic resonance (NMR) that when a constant linear gradient field was applied in a pulse sequence with two rf pulses applied at times 0 and τ [1], unexpected multiple echoes were observed at times $2\tau, 3\tau, 4\tau, \ldots$ [2], instead of having a single echo at time 2τ as predicted by the early study. This phenomenon was later found to be the effect of a distant dipolar field (DDF) [3], or in an equivalent term, intermolecular multiple-quantum coherence (iMQC) [4–6], in the sample.

The distant dipolar field, also historically called the demagnetization field, is the spin–spin interaction between different molecules in a sample. Before gradients were commonly used in NMR pulse sequences, distant dipolar field effects were not observed mainly because of low static field strength B_0 and poor field homogeneity. In liquid, the magnitude of the DDF signal is only about 1% of the full magnetization at 60 MHz, and is proportional to the field strength. With present field strengths and excellent field homogeneity, the DDF signal becomes observable when a pair of asymmetric pulsed field gradient is applied to suppress the conventional signal.

* Corresponding author. Fax: +1 585 273 4518.
E-mail address: jianhui.zhong@rochester.edu (J. Zhong).

1090-7807/$ - see front matter © 2007 Elsevier Inc. All rights reserved.
doi:10.1016/j.jmr.2006.12.017

Over the past decade, however, there has been an increasing interest in studying the signal formed under the influence of the distant dipolar field. The most extensively used pulse sequence is the so-called correlation spectroscopy revamped by asymmetric z-gradients echo detection (CRAZED) sequence [4], as shown in Fig. 1. The signal produced by the sequence exhibits interesting relaxation, diffusion, and structural properties [7–17], and provides contrast for magnetic resonance imaging (MRI) that is fundamentally different from that by conventional techniques [18–24]. Nevertheless, applications of such signal have been severely limited by its small amplitude in most tissues primarily due to transverse relaxation, despite the fact that some improvement can be obtained, for example, with simultaneous acquisition of multiple orders of quantum coherence [25,26]. The signal intensity is generally only a fraction of the full magnetization (typically a few percent at $B_0 = 9.4$ T). It is noted however, unlike the conventional signal which drops monotonically due to T_2 decay, the signal formed under the distant dipolar field rises initially as $t\exp(-t/T_2)$ [27]. Therefore, multiecho acquisitions such as in echo-planar or fast spin-echo imaging during the rising period of the signal may have the potential to substantially increase efficiency in data acquisition and compensate to some degree for its intrinsic low signal magnitude. Another reason that the sequence with multi spin-echo is analyzed is because the sequence also has the potential to eliminate macroscopic susceptibility artifacts.

In this paper, we analyze the signal formed in the pulse sequence as shown in Fig. 1. The pulse sequence is composed of a CRAZED sequence, which is used to prepare the iMQC signal, and a multiple spin-echo sequence that consists of a series of refocusing π pulses with finite pulse width. In particular, we focus on the scenario where the area of the second gradient field is twice of that of the first ($|G_2\delta_2| = -2|G_1\delta_1|$), so that the second-order echo or the intermolecular double-quantum coherence (iDQC) signal is selected.

Various aspects of effective implementation of multiecho acquisitions in the presence of distant dipolar fields are discussed by Kennedy et al. [28]. Experiments were performed to investigate the influence of closely spaced π pulses on the iDQC signal formation and the implications for practical multiecho acquisitions. It was found that as the ratio of the pulse duration over the pulse separation increases, the formation of the iDQC signal is attenuated. This paper provides the theoretical explanations to the experimental observations and studies in detail the influence of the closely spaced refocusing π pulses on the iDQC signal formation.

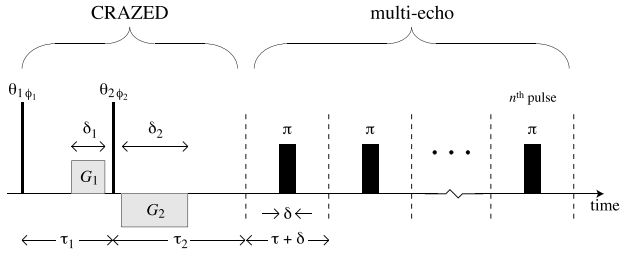

Fig. 1. The pulse sequence considered in this paper. It is composed of two parts: the CRAZED sequence ($|G_2\delta_2| = -2|G_1\delta_1|$) that prepares the dipolar field signal, and the multiple spin-echo sequence consisting of a series of π pulses that refocus the signal. In the figure, δ is the pulse duration of the refocusing pulses, τ is the free evolution time between the refocusing pulses, and $\tau + \delta$ is the pulse separation.

The dipolar field and transverse relaxation are taken into consideration in the Bloch equation throughout our analysis. Magnetization during a single rf pulse is first solved to the first order of the dipolar field in Section 2. The evolution of magnetization between the π pulses and the initial magnetization of the multiple spin-echo sequence are then discussed in Section 3. The magnetization during the multiple spin-echo sequence is calculated by repeatedly applying these results. The features of the transverse magnetization under the influences of the dipolar field and the transverse relaxation for the first few pulses in the multiple spin-echo sequence are discussed in detail in Section 4. The expressions for the magnetization for arbitrary number of pulses in the multiple spin-echo pulse sequence are obtained for the long T_2 limit in Section 5. We will see from the analysis that because of the finiteness of the π pulses, the magnetization is rephased due to the dipolar field not only during the CRAZED sequence, but also during the multiple spin-echo sequence. Moreover, we will see the reason why the iDQC signal rises less when it undergoes shorter free evolution time, and will study the signal dependence on the phase of the rf pulses. The comparison between the calculations and the experiment is given in Section 6. Finally, in Section 7, we will estimate the optimal number of π pulses for achieving maximal total acquired signal using parameters for water, brain white matter, and muscle. Selection of these parameters covers a large range of typical transverse relaxation times in tissues.

It is remarked that we have adopted an analytical approach to tackle the problem. It has the great advantage that the equations immediately show which parameter has a large effect, and suggest the origins of the observed signals. To make an analytical approach possible, we have to make first-order approximations so that the calculations are tractable. The dipolar field is a small effect in most biological tissues. As will be shown in the following sections, the relative magnitude of the DDF is in the order of 0.1 or less in comparison to the rf pulses. The first-order approximations used in this work are analyzed using typical experimental parameters, and are justified with a good agreement between the theory and the experiment. This is in contrast to numerical methods from the start, such as that in [29,30], in which rf irradiation, radiation damping, molecular diffusion, relaxation, and dipolar field can be taken into account "exactly" but leaving all physical mechanisms subtle.

2. Magnetization during a finite rf pulse

We first consider the effect of finite duration of an rf pulse on the magnetization evolution. In the laboratory

frame, a linearly polarized rf pulse along the direction $\hat{e}_\phi = \cos\phi\hat{x} + \sin\phi\hat{y}$ in the transverse plane can generally be written as $\vec{B}_{\mathrm{rf,lab}}(\vec{r},t) = 2C(\vec{r},t)\cos\omega_{\mathrm{rf}}t[\cos\phi\hat{x} + \sin\phi\hat{y}]$, where ω_{rf} is the frequency of the rf pulse. The pulse envelope function $C(\vec{r},t)$ is assumed to be a constant in this paper ("hard" pulse assumption), i.e., $C(\vec{r},t) = C$ during the pulse. In the rotating frame of frequency ω_{rf}, the rf pulse can be approximated as $\vec{B}_{\mathrm{rf}}(\vec{r},t) \approx C(\cos\phi\hat{x} + \sin\phi\hat{y})$ [31]. The evolution of the magnetization $\vec{M}$ for a spin-$\frac{1}{2}$ system during the rf pulse is governed by the Bloch equation, which in the rotating frame of resonance frequency is given by

$$\frac{\mathrm{d}}{\mathrm{d}t}\vec{M} = \gamma\vec{M}\times(\vec{B}_{\mathrm{rf}} + \vec{B}_{\mathrm{d}}) - \frac{1}{T_2}(M_x\hat{x} + M_y\hat{y}), \tag{1}$$

where γ is the gyromagnetic ratio, T_2 is the transverse relaxation time, and $\vec{B}_{\mathrm{d}}$ is the dipolar field. Note that diffusion is not considered in Eq. (1) explicitly. For water and typical tissues studied in this work, the diffusion coefficient D is around $2.3\times10^{-9}\ \mathrm{m^2\,s^{-1}}$ at biological temperature, so the spin molecules diffuse by a distance of $\sqrt{2DT} \approx 7\ \mu\mathrm{m}$ in the CRAZED sequence of time scale $T \sim 10$ ms. A gradient field with field strength 22 mT/m and duration 2 ms results in a correlation length of about 85 μm. Therefore, diffusion can be ignored in the CRAZED part of the pulse sequence in Fig. 1. In the multiple spin-echo part, diffusion is taken into account only through the shortened effective T_2 for simplicity. Even though the effects of diffusion on iMQC signals differ for different orders of iMQC during its evolution, during the detection period when only detectable conventional single-quantum signal needs to be considered, the above approximation should apply to this detectable signal. Since the longitudinal relaxation time T_1 is much longer than the time period we are focusing on, its effect on the magnetization evolution is also ignored.

For uniform magnetization or magnetization modulated by a gradient along a particular direction, the dipolar field $\vec{B}_{\mathrm{d}}$ is given by a simple form [3,27]:

$$\vec{B}_{\mathrm{d}} = \frac{\mu_0}{3}A[3(\vec{M}\cdot\hat{z})\hat{z} - \vec{M}]. \tag{2}$$

Here μ_0 is the permeability in vacuum and A is a constant depending on the form of the magnetization. In this paper, the pulse field gradients are assumed to be substantially stronger than the intrinsic inhomogeneity of the sample. The local magnetic field variations can then be ignored. This assumption is also valid when sample of water was used in the experiment. Since the magnetization during the multiple spin-echo sequence has a functional form $\vec{M}(\vec{r}) = \vec{F}(\hat{G}\cdot\vec{r})$ where $\hat{\mathrm{G}}$ is a constant vector in the direction of the gradient field, we have $A = -[3(\hat{G}\cdot\hat{z})^2 - 1]/2$.

With the dipolar field expressed in the form (2), Eq. (1) can be rewritten as:

$$\frac{\mathrm{d}}{\mathrm{d}t}M_\pm(t) \mp \mathrm{i}\gamma C\,\mathrm{e}^{\pm\mathrm{i}\phi}M_z(t) + \frac{1}{T_2}M_\pm(t) = \mp\mathrm{i}A\gamma\mu_0 M_z(t)M_\pm(t) \tag{3a}$$

and

$$\frac{\mathrm{d}}{\mathrm{d}t}M_z(t) - \frac{\mathrm{i}}{2}\gamma C[\mathrm{e}^{-\mathrm{i}\phi}M_+(t) - \mathrm{e}^{\mathrm{i}\phi}M_-(t)] = 0, \tag{3b}$$

where $M_\pm = M_x \pm \mathrm{i}M_y$. It should be noted that the magnetization in Eq. (3) contains the spatial dependence $\hat{G}\cdot\vec{r}$. Since such spatial dependence does not affect the time evolution of magnetization in Eq. (3), it is not written explicitly for simplicity. The dipole coupling factor $\gamma\mu_0 M_z$ on the right-hand side of Eq. (3) causes a rotation on $\vec{M}(t)$. The magnitude of this factor is approximately $\gamma\mu_0 M_0$, where M_0 is the equilibrium magnetization. If the dipolar field effect in Eq. (3) is ignored, the equation can be exactly solved. When the dipolar field effect is taken into account, $\vec{M}(t)$ can be iterated into a series of all orders of dipolar field. The terms that underwent n dipolar field interactions have the amplitude approximately proportional to g^n, where

$$g = A\gamma\mu_0 M_0\delta \tag{4}$$

and δ is the pulse duration. To the first order of the dipolar field, i.e., first order of g, the truncation error in $M(t)$ is of order g^2. It increases with the pulse duration, or the inverse of the pulse strength. However, even when δ goes up to 10 ms at $B_0 = 9.4$ T, the truncation error is only about 1%. At lower static field, δ can be even longer without causing severe error truncation. Therefore, solving Eq. (3) with a linear dipolar field approximation is valid in the time scales of typical MRI experiments. To first order of the dipolar field, the magnetization reads as

$$M_\pm(t) \simeq M_\pm^{(0)}(t) + M_\pm^{(1)}(t) \quad \text{and}$$
$$M_z(t) \simeq M_z^{(0)}(t) + M_z^{(1)}(t), \tag{5}$$

where $\vec{M}^{(0)}$ and $\vec{M}^{(1)}$ are, respectively, the zeroth- and first-order solutions of the magnetization.

We begin by considering the limit where we can ignore the DDF, Eq. (3) gives

$$\frac{\mathrm{d}}{\mathrm{d}t}M_\pm^{(0)}(t) = \pm\mathrm{i}\gamma C\,\mathrm{e}^{\pm\mathrm{i}\phi}M_z^{(0)}(t) - \frac{1}{T_2}M_\pm^{(0)}(t) \tag{6a}$$

and

$$\frac{\mathrm{d}}{\mathrm{d}t}M_z^{(0)}(t) = \frac{\mathrm{i}\gamma C}{2}\left[\mathrm{e}^{-\mathrm{i}\phi}M_+^{(0)}(t) - \mathrm{e}^{\mathrm{i}\phi}M_-^{(0)}(t)\right]. \tag{6b}$$

Note that if the rf pulse duration is much shorter than T_2, so that the transverse relaxation can be ignored, Eq. (6) gives the magnetization after the rf pulse as $(M_x, M_y, M_z)_{\mathrm{after}} = R(\theta,\phi)(M_x, M_y, M_z)_{\mathrm{before}}$, where

$$R(\theta,\phi) = \begin{bmatrix} \cos^2\frac{\theta}{2} + \sin^2\frac{\theta}{2}\cos 2\phi & \sin^2\frac{\theta}{2}\sin 2\phi & -\sin\theta\sin\phi \\ \sin^2\frac{\theta}{2}\sin 2\phi & \cos^2\frac{\theta}{2} - \sin^2\frac{\theta}{2}\cos 2\phi & \sin\theta\cos\phi \\ \sin\theta\sin\phi & -\sin\theta\cos\phi & \cos\theta \end{bmatrix}. \tag{7}$$

In this case, the rf pulse rotates the magnetization by an angle $\theta = \gamma Ct$ about the direction $\hat{e}_\phi = \cos\phi\hat{x} + \sin\phi\hat{y}$. If $\theta = \pi$, the magnetization after the rf pulse reduces to

$$M_z = -M_{z\ \text{before}} \quad \text{and} \quad M_\pm = e^{\pm 2i\phi} M_{\mp\ \text{before}}. \tag{8}$$

Eqs. (6a) and (6b) can be combined into two second-order linear differential equations in $M_\pm^{(0)}(t)$, which can be solved with diagonalization transformation. With the initial values of the magnetization just before the rf pulse taken as $M_\pm^{(0)}(0) = M_{\pm 0}$ and $M_z^{(0)}(0) = M_{z0}$, the zeroth-order transverse magnetization becomes

$$M_\pm^{(0)}(t) = c_1(t) M_{\pm 0} + c_2(t)\, e^{\pm 2i\phi} M_{\mp 0} \pm c_3(t)\, e^{\pm i\phi} M_{z0}. \tag{9}$$

The zeroth-order longitudinal magnetization can be found by solving (6b) with the substitution of (9):

$$M_z^{(0)}(t) = \frac{c_3(t)}{2}\left[e^{-i\phi} M_{+0} - e^{i\phi} M_{-0}\right] + c_4(t) M_{z0}. \tag{10}$$

The coefficients in (9) and (10) are

$$c_1(t) = \frac{1}{2} e^{-\frac{t}{2T_2}}\left[e^{-\frac{t}{2T_2}} + \cosh\frac{a_0 t}{2T_2} - \frac{1}{a_0}\sinh\frac{a_0 t}{2T_2}\right], \tag{11a}$$

$$c_2(t) = \frac{1}{2} e^{-\frac{t}{2T_2}}\left[e^{-\frac{t}{2T_2}} - \cosh\frac{a_0 t}{2T_2} + \frac{1}{a_0}\sinh\frac{a_0 t}{2T_2}\right], \tag{11b}$$

$$c_3(t) = \frac{2i}{a_0}\gamma C T_2\, e^{-\frac{t}{2T_2}}\sinh\frac{a_0 t}{2T_2}, \tag{11c}$$

$$c_4(t) = e^{-\frac{t}{2T_2}}\left[\cosh\frac{a_0 t}{2T_2} + \frac{1}{a_0}\sinh\frac{a_0 t}{2T_2}\right], \tag{11d}$$

where $a_0 = \sqrt{1 - (2\gamma C T_2)^2}$. In most situations, $2\gamma C T_2 \gg 1$. Substituting $\gamma C\delta = \pi$ for a π pulse of duration δ and ignoring the second-order terms $O(\frac{\delta}{T_2})^2$ in a_0, we get $a_0 \approx 2i\gamma C T_2$. Then to the first order of δ/T_2, Eq. (11) at the end of the π pulse becomes

$$c_1(\delta) \approx -\frac{\delta}{4T_2}, \quad c_2(\delta) \approx 1 - \frac{3\delta}{4T_2}, \quad c_3(\delta) \approx 0, \quad \text{and}$$
$$c_4(\delta) \approx -\left(1 - \frac{\delta}{2T_2}\right). \tag{12}$$

We can see from Eqs. (9) and (10) that there is a mutual exchange in $M_\pm$ and M_z with the same time varying amplitude $c_3(t)$ during the pulse. To the first order of δ/T_2, $c_3(\delta) \approx 0$. This means that the exchange between $M_\pm$ and M_z vanishes at the end of the π pulse. The coefficient $c_2(t)$ associates with a flipping from $M_\pm$ to $M_\mp$, and $c_1(t)$ associates with the residual amplitude in $M_\pm$. The coefficient $c_4(t)$ associates with a flipping from M_z to $-M_z$. It should be noted that for sample with large T_2 like water, $c_1(\delta) \sim (\delta/T_2)c_2(\delta)$, and is much smaller than $c_2(\delta)$.

When there is no T_2 relaxation during the pulse, $M_\pm$ is flipped into $M_\mp$ and M_z into $-M_z$. In this case, $c_1(\delta) = c_3(\delta) = 0$, $c_2(\delta) = 1$, and $c_4(\delta) = -1$. When T_2 relaxation is considered, according to the Bloch equations $d\vec{M}/dt = \gamma\vec{M} \times \vec{B} - (\vec{M}_x + \vec{M}_y)/T_2$, the effective precession frequency in the presence of refocusing pulses is decreased in the presence of T_2 relaxation. Consequently, $M_\pm$ and M_z do not completely flip into $M_\mp$ and $-M_z$, and transverse relaxation causes the incomplete flipping of $M_\pm$ and M_z as shown in (9) and (10).

According to Eq. (3), the magnetization to the first-order dipolar field effect during the refocusing pulse in the multiple spin-echo sequence is given by

$$\frac{d}{dt}M_\pm^{(1)}(t) = \pm i\gamma C e^{\pm i\phi} M_z^{(1)}(t) \mp iA\gamma\mu_0 M_z^{(0)}(t) M_\pm^{(0)}(t) - \frac{M_\pm^{(1)}(t)}{T_2} \tag{13a}$$

and

$$\frac{d}{dt}M_z^{(1)}(t) = \frac{i}{2}\gamma C\left[e^{-i\phi} M_+^{(1)}(t) - e^{i\phi} M_-^{(1)}(t)\right]. \tag{13b}$$

Similar to the zeroth-order equations, Eqs. (13a) and (13b) can be combined into two second-order linear differential equations in $M_\pm^{(1)}(t)$, which can be solved with diagonalization transformation. Here the initial values of the perturbed magnetization just before the rf pulse is zero, i.e. $M_\pm^{(1)}(0) = 0$ and $M_z^{(1)}(0) = 0$. We have then

$$\begin{aligned} M_\pm^{(1)}(t) = A\gamma\mu_0 T_2 \Big\{ & \pm d_1(t) M_{z0} M_{\pm 0} \pm d_2(t)\, e^{\pm 2i\phi} M_{z0} M_{\mp 0} \\ & + d_3(t)\, e^{\mp i\phi} M_{\pm 0}^2 + d_4(t)\, e^{\pm 3i\phi} M_{\mp 0}^2 \\ & + d_5(t) e^{\pm i\phi} M_{+0} M_{-0} + d_6(t) e^{\pm i\phi} M_{z0}^2 \Big\}. \end{aligned} \tag{14}$$

Substituting $M_\pm^{(1)}(t)$ into Eq. (13b), we get

$$\begin{aligned} M_z^{(1)}(t) = A\gamma\mu_0 T_2 \Big\{ & d_7(t) M_{z0}\left[e^{-i\phi} M_{+0} + e^{i\phi} M_{-0}\right] \\ & + d_8(t)\left[e^{-2i\phi} M_{+0}^2 - e^{2i\phi} M_{-0}^2\right] \Big\}. \end{aligned} \tag{15}$$

The coefficients d_i with $i = 1$–8 are given in Appendix A. Again, ignoring the second-order terms $O(\frac{\delta}{T_2})^2$, Eq. (A.1) at $t = \delta$ becomes

$$d_1(\delta) \approx d_2(\delta) \approx 2d_8(\delta) \approx \frac{i}{4}\frac{\delta}{T_2} \quad \text{and}$$
$$d_3(\delta) \approx d_4(\delta) \approx d_5(\delta) \approx d_6(\delta) \approx d_7(\delta) \approx 0. \tag{16}$$

The rf pulse causes an exchange between the transverse and longitudinal magnetization under the transverse relaxation. At each moment during the pulse, the longitudinal component of the magnetization affects the evolution of the transverse component through the dipole interaction. The first-order transverse magnetization in (14) indicates dipolar field interaction of two different origins. The first origin comes from the direct interaction between M_{z0} and $M_{\pm 0}$. During the pulse, $M_{\pm 0}$ evolves under the influence of M_{z0} through the dipolar field interaction. The direct interaction between M_{z0} and $M_{\pm 0}$ in (14) is indicated by the terms with $d_1(t)$ and $d_2(t)$. The second origin comes from the self interactions of M_{z0} and $M_{\pm 0}$. In this case, part of M_{z0} rotates into the transverse plane and this component evolves under the influence of its remaining amplitude in the longitudinal direction through the dipolar field interaction. In the same way, part of $M_{\pm 0}$ rotates into the longitudinal direction which affects the evolution of its remaining amplitude on the transverse plane through the dipolar field interaction. The self interactions of M_{z0} and $M_{\pm 0}$ in (14) are identified by the terms with $d_3(t)$, $d_4(t)$, $d_5(t)$, and $d_6(t)$. On the other hand, the dipolar field does not directly interact with M_z, but its effect comes to M_z from $M_\pm$ through the rotation by the rf pulse (see Eq. (13b)). Therefore, in Eq. (15), we can interpret $d_7(t)$ as the direct interaction and $d_8(t)$ as

the self interaction for $M_z^{(1)}$. Note also that $M_z^{(1)}$ has no dependence on $M_{+0}M_{-0}$ and M_{z0}^2 because they are canceled in Eq. (13b).

In summary, the zeroth-order solutions and first-order solutions are given by Eqs. (9)–(11) and (14), (15), (A.1), respectively. It can be seen from the solutions that the longitudinal and transverse magnetizations are mixed with each other after passing through the rf pulse. This mixing is introduced by both the transverse relaxation ($c_i(t)$) and the dipolar field effect ($d_i(t)$). If the dipolar field effect is excluded by setting $d_i(t) = 0$ for all i and the relaxation time T_2 is set to be infinite during the pulse, there will be no mixing between the longitudinal and transverse magnetizations after passing through the π pulse just as described in Eq. (8).

3. Dipolar field signal in a multiple spin-echo sequence

The Bloch equation describing the magnetization *between* the refocusing π pulses in the rotating frame is given by

$$\frac{dM_z(t)}{dt} = 0$$

and

$$\frac{dM_\pm(t)}{dt} = \mp iA\gamma\mu_0 M_z(t)M_\pm(t) - \frac{1}{T_2}M_\pm(t). \tag{17}$$

Then the magnetization between two π pulses reads as

$$M_z(t) = M_z(t_0)$$

and

$$M_\pm(t) = M_\pm(t_0)\, e^{-\frac{(t-t_0)}{T_2}} e^{\mp iA\gamma\mu_0 M_z(t_0)(t-t_0)}, \tag{18}$$

where t_0 is the time right after the previous π pulse.

The magnetization throughout a multiple spin-echo sequence is then calculated by repeatedly applying Eq. (5) for the time during the π pulses and Eq. (18) for the free evolution outside the π pulses. The initial condition of the magnetization at the beginning of the multiple spin-echo train is given by the magnetization at the end of the CRAZED sequence, i.e., $\vec{M}(\tau_1 + \tau_2)$. Without loss of generality, the phase of the second rf pulse of the CRAZED sequence (ϕ_2) is chosen as the reference phase of the other pulses and is taken as $\phi_2 = 0$. Also the flip angle of the first rf pulse (θ_1) is taken to be 90° in order to maximize the iDQC signal. Then the longitudinal and transverse magnetizations at the end of the CRAZED sequence are given by [27,32]:

$$M_z(\tau_1 + \tau_2) = -M_0 \sin\theta_2\, e^{-\frac{\tau_1}{T_2}} \cos\alpha, \tag{19a}$$

$$M_\pm(\tau_1 + \tau_2) = \mp iM_0\, e^{-\frac{\tau_1+\tau_2}{T_2}} \times e^{\mp i\beta}\left[e^{\pm i\alpha}\cos^2\frac{\theta_2}{2} - e^{\mp i\alpha}\sin^2\frac{\theta_2}{2}\right], \tag{19b}$$

where θ_2 is the flip angle of the second rf pulse. The parameters α and β are, respectively, the total phases acquired in the first and the second evolution periods (τ_1, τ_2) of the CRAZED sequence, which are given by

$$\alpha \equiv \phi_1 - \gamma\vec{G}_1 \cdot \vec{r}\delta_1$$

and

$$\beta \equiv \gamma\vec{G}_2 \cdot \vec{r}\delta_2 + A\gamma\mu_0 M_z(\tau_1^+)\tau_2. \tag{20}$$

Here ϕ_1 is the phase of the first rf pulse, and $M_z(\tau_1^+) = M_z(\tau_1 + \tau_2)$.

4. Magnetization evolution for the first few refocusing pulses

To obtain iDQC signal, the area of the second gradient pulse in the CRAZED sequence is taken to be twice of the first gradient, i.e., $G_2\delta_2 = -2G_1\delta_1$. In this paper, signals for water, muscle, and brain white matter are calculated with the transverse relaxation T_2 and the proton number density n_H summarized in Table 1. Since the transverse relaxations of the muscle and the white matter are of about the same order of magnitude when compared with the considered evolution time, discussion in the following will only use water and muscle as examples. The signal for the white matter will be discussed in detail in the last section of this paper, when differences of other characteristics of these tissues are considered.

As discussed in Section 2, the rf pulse causes an exchange between the transverse and longitudinal magnetization under the influence of transverse relaxation. The terms with both balanced phase, i.e., $\exp[ip(\gamma\vec{G}_1 \cdot \vec{r}\delta_1)]$ with $p = 0$, and unbalanced spatially dependent phase ($p = \pm1, \pm2, \ldots$) of $M_\pm$ introduced by the pair of gradient fields in the CRAZED sequence enter into M_z, and vice versa, during the π pulses. However, the part of magnetization with the unbalanced phase is spatially averaged out when the signal from the whole sample is summed, so only the part with the balanced phase is observable.

In Fig. 2 we show the normalized spatially averaged transverse magnetization ($|M_+|/M_0$), based on the repeated applications of Eqs. (5) and (18) and the parameters listed in Table 1, for the first five refocusing pulses for water and muscle with the phase of the pulses ϕ taken as zero. Note that the magnetization during the rf pulses are shown explicitly in the shaded regions. The parameter r in the plots is the ratio of the pulse duration to the pulse separation given by

$$r = \frac{\delta}{\tau + \delta}, \tag{21}$$

Table 1
Parameters used at $B_0 = 9.4$ T for the calculations of this paper

Sample	T_2 (ms)	n_H (of H_2O)
Doped water	400	0.9
White matter	40	0.7
Muscle	21	0.8

The T_2 of doped water is measured from the experiment in this paper, and the T_2 of muscle is measured experimentally in Ref. [33].

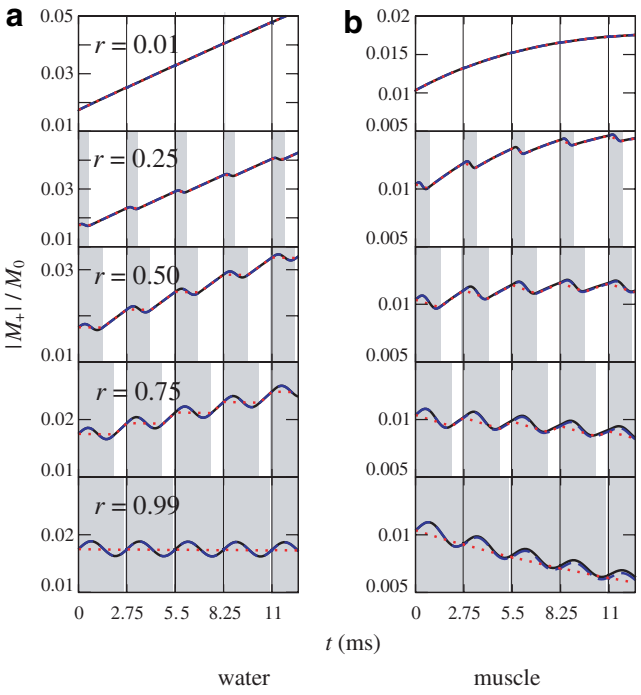

Fig. 2. The calculated magnitude of the transverse magnetization that is spatially averaged and normalized to M_0 against time for (a) water ($T_2 = 400$ ms) and (b) muscle ($T_2 = 21$ ms) from Eqs. (5) and (18). The shades in the figure denote the time periods when the refocusing π pulses are applied. The solid lines show the evolution of $|M_+|$ with both the transverse relaxation and the dipolar field effect taken into account during the rf pulse, and the dotted lines show the evolution of $|M_+|$ with the dipolar field effect considered only during the free evolution period. We also calculate the approximations of magnetizations by ignoring the interactions with nonlinear $\frac{\delta}{T_2}$ dependence (Section 5). The approximated results are shown in dashed lines. $\tau_1 = 1.5$ ms, $\tau_2 = 6$ ms, $\phi = \phi_1 = 0$, and $\tau + \delta$=2.75 ms have been used in the calculations.

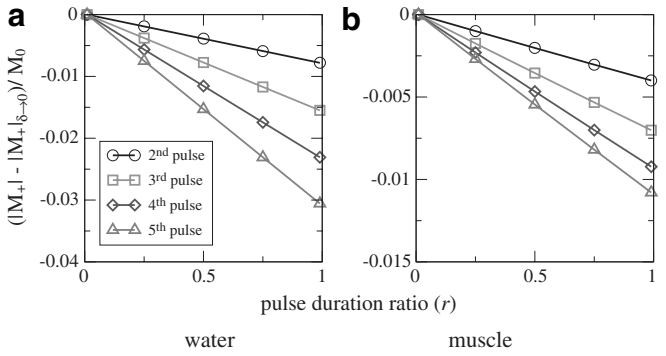

Fig. 3. The calculated change in the magnitude of the normalized spatially averaged transverse magnetization as a function of the pulse duration to pulse separation ratio r at the times just before the application of the π pulses. (a) is for water and (b) is for muscle samples.

where δ is the duration of a refocusing pulse in the multiple spin-echo sequence, and τ is the free evolution time between two consecutive refocusing pulses. The lines with $r = 0.01$ correspond to the sequences with very short π pulses. These lines show the unique rising of iDQC signal during the free evolution periods between the pulses as have been elucidated in Ref. [27]. For instantaneous π pulses, the iDQC signal rises as $t\exp(-t/T_2)$. When the duration of the π pulses becomes longer (wider shaded regions), the transverse magnetization undergoes less free evolution time (narrower unshaded regions). The finiteness of the π pulses decreases the time during which the signal can rise, so that the amplitude of the signals with longer pulses increases less than that with instantaneous pulses. Since the rising rates of the signal with different δ are more or less the same in the free evolution periods, the amount of signal drop after passing through n finite π pulses is linear in the pulse duration δ, as shown in Fig. 3 where the relative signal $(|M_+| - |M_+|_{\delta\to 0})/M_0$ is plotted as a function of r. For water, the signal also drops linearly with the number of pulses n. This observation will be further proved analytically in Section 6. In the situation when the pulses occupy nearly the whole evolution period, $|M_+|$ almost undergoes no free evolution and the signal stops to rise. The lines with $r = 0.99$ in Fig. 2 show the oscillation of the transverse magnetization during the pulse with the envelope governed by T_2 decay. This decay is clearly shown when comparing $|M_+|$ for water and muscle in the figures. In fact we will see later in Eq. (27) that for $\tau \approx 0$, $|M_+|$ evaluated at the end of the nth pulse is proportional to $\exp(-n\delta/T_2)$.

The effect of the dipolar field on $|M_+|$ during the pulse can be examined by comparing the above with the case when the dipolar effect is excluded from the calculation during the pulse (setting $d_i(t) = 0$, $i = 1, \ldots, 8$). The results are plotted as dotted lines in Fig. 2. It can be seen from the figure that other than the disappearance of the oscillations of $|M_+|$ during the pulses, there is no change in $|M_+|$ at the regions between the pulses, except when $n\delta \sim T_2$ where n is the pulse number. During the refocusing pulse, the dipolar field effect in the first half of the pulse is reversed during the second half of the pulse, so that the signal measured does not reflect this effect in the pulse. However, when $\phi \neq 0$, we shall see that the measured signal does depend on the dipolar field effect during the pulse. This will be examined in the next section.

According to Eqs. (12) and (16), the coefficients $c_3(\delta)$, $d_3(\delta)$, $d_4(\delta)$, $d_5(\delta)$, $d_6(\delta)$, and $d_7(\delta)$ are at least second order in δ/T_2. Thus they are very small when T_2 is large and we can ignore their corresponding interactions on $\vec{M}$. In Fig. 2, we plot $|M_+|$ under this approximation for water and muscle in dashed lines. The approximated values of $|M_+|$ coincide with the exact calculations (the solid lines) except for the muscle with large r. The truncation error of ignoring these coefficients increases with t, but is still negligible when $t \sim 0.5\ T_2$. Therefore, without missing any significant interaction, this approximation can be used to describe the evolution picture of $M_\pm$.

5. Magnetization evolution for arbitrary number of refocusing pulses

In this section, we calculate the transverse and longitudinal magnetizations during the free evolution time for

arbitrary number of refocusing pulses in the long T_2 limit ($\delta/T_2 \ll 2\pi$). The approximation of ignoring the interactions with second- or higher-order dependence on δ/T_2 as discussed in the end of the last section enables us to write down the analytic form of the magnetization explicitly. In this way one can analyze the cumulative effect of the finiteness of the refocusing pulses on the magnetization. Moreover the expressions show how the signal depends on the phase of the refocusing pulses. On the other hand, we have also calculated the transverse and longitudinal magnetizations during the refocusing pulses for arbitrary number of pulses in the long T_2 limit. However, since no measurement is carried out during the pulses, the expressions for $\vec{M}$ during the refocusing pulses will not be discussed in this paper.

As discussed in Section 4, we apply Eqs. (5) and (18) repeatedly in the multiple spin-echo sequence. Here we ignore the interactions with nonlinear dependence on δ/T_2 and keep terms to the first order of dipolar field. After some straightforward but tedious algebra, the spatially averaged magnetization after the nth π pulse is given by:

$$M_{\pm,n}(t) \approx -\frac{e^{\pm i\phi} m_1 \omega_d}{2} \times \left\{ \sum_{m=0}^{n} e^{\mp(-1)^m i(\phi-2\phi_1)} c_1(\delta)^{n-m} c_2(\delta)^m F_1(n,m) + i\sum_{m=0}^{n-1} c_1(\delta)^{n-1-m} c_2(\delta)^m K_{m\pm}(\delta) F_2(n-1,m) \right\} e^{-\frac{t+\left(n-\frac{1}{2}\right)\tau}{T_2}}, \tag{22a}$$

$$M_{z,n}(t) \approx 0, \tag{22b}$$

with

$$F_1(n,m) = \sum_{j=1}^{C_m^n} \left[\left(\tau_2 + \frac{\tau}{2}\right) + \left[\sum_{k=1}^{n-1} (-1)^{\sum_{l=1}^{k} q_{nmjl}} c_4(\delta)^k \right] \tau + (-1)^m c_4(\delta)^n t \right], \tag{23a}$$

$$F_2(n,m) = \sum_{j=1}^{C_m^n} \left\{ 1 + \left[\sum_{k=1}^{n} (-1)^{\sum_{l=1}^{k} q_{nmjl}} c_4(\delta)^k \right] \right\} T_2, \tag{23b}$$

$$K_{m\pm}(t) = e^{\mp(-1)^m i(\phi-2\phi_1)} d_1(t) - e^{\pm(-1)^m i(\phi-2\phi_1)} d_2(t), \tag{23c}$$

where ϕ is the phase of the π pulses, $\omega_d = -A\gamma\mu_0 M_0 \sin\theta_2 \exp(-\tau_1/T_2)$ is the frequency due to the dipolar field, and $m_1 = M_0 \cos^2(\theta_2/2)\exp[-(\tau_1+\tau_2)/T_2]$ is the conventional signal amplitude (i.e., $G_2\delta_2 = -G_1\delta_1$) of the CRAZED sequence. The time t in Eq. (22) is counted from the end of the previous π pulse. Hence the time in the middle of two successive π pulses when the signal is acquired is $t = \tau/2$. The function $K_{m\pm}$ in Eq. (23c) shows the dipolar field effect during the pulse through the interactions of $d_1(t)$ and $d_2(t)$. At the end of the pulse, it can be approximated as

$$K_{m\pm}(\delta) \approx \pm\frac{(-1)^m}{2}\frac{\delta}{T_2}\sin(\phi - 2\phi_1). \tag{24}$$

We have deliberately kept $c_1(\delta)$, $c_2(\delta)$, $c_4(\delta)$, $d_1(\delta)$, and $d_2(\delta)$ explicit in Eqs. (22) and (23). This enables us to evaluate the effects of different terms on the rephasing of $\vec{M}$ by the dipolar field at different time.

According to Eq. (9), $c_1(\delta)$ and $c_2(\delta)$ associate with the flipping of $M_\pm$. The power m of $c_2(\delta)^m$ in Eq. (22a) shows the number of times that $M_\pm$ is flipped to $M_\mp$ after interacting with n refocusing pulses in the pulse sequence, and the power m' of $c_1(\delta)^{m'}$ shows the number of times that $M_\pm$ remains unchanged. In Eq. (23), $\{q\}$ is defined as the set of permutations that record all the flipping orders of $M_\pm$ to $M_\mp$, and q_{nmjl} is the lth element of the jth permutation with m flips and $(n-m)$ unflips. The value of $q_{nmjl} = 1$ when $M_\pm$ is flipped to $M_\mp$ after interacting with the refocusing pulse, and $q_{nmjl} = 0$ when $M_\pm$ remains unchanged. The details of the evaluation of $\{q\}$ are given in Appendix B. Similar to the roles of $c_1(\delta)$ and $c_2(\delta)$ in the case of $M_\pm$, $c_4(\delta)$ associates with the change of M_z to $-M_z$. Then the power k of $c_4(\delta)^k$ in Eq. (23) shows the number of times that M_z is flipped to $-M_z$ after interacting with n pulses in the pulse sequence. Therefore, the terms with $c_4(\delta)^k$ correspond to the rephasing of $M_\pm$ by the dipolar field that happens after the kth pulse.

5.1. Rephasing of $M_\pm$ that happened during the free evolution period

During the free evolution period between the π pulses, parts of $M_\pm$ with the unbalanced spatially dependent phase are rephased by the dipolar field (see Eq. (18)). The first sum of Eq. (22a) shows the rephasing process of $M_\pm$ that happened during the free evolution period. The first term of $F_1(n,m)$ corresponds to the rephasing of $M_\pm$ during the free evolution period before the first refocusing pulse of the multiple spin-echo sequence, and the remaining terms with $c_4(\delta)^k$ correspond to the rephasing of $M_\pm$ during the free evolution period between the kth and the $(k+1)$th refocusing pulses of the multiple spin-echo sequence.

The amplitude of the first sum in Eq. (22a) depends on the value of the free evolution time τ between two π pulses, and the parameters $c_1(\delta)$, $c_2(\delta)$, and $c_4(\delta)$. When $n\tau \ll T_2$, the amplitude increases linearly with τ. In order to show the amplitude dependence on the constants $c_1(\delta)$, $c_2(\delta)$, and $c_4(\delta)$, the first sum of Eq. (22a), together with $c_2(\delta)$ and $c_4(\delta)$ (where $c_1(\delta) = \exp(-\delta/T_2) - c_2(\delta)$), are plotted in Fig. 4. Note that the first sum does not explicitly depend on the decay factor $\exp(-t/T_2)$. The decrease in its value comes solely from the incomplete flipping of $\vec{M}$ by the refocusing pulses under the T_2 decay, as represented by $c_1(\delta)$, $c_2(\delta)$, and $c_4(\delta)$. It can be seen in the figure that for a fixed free evolution time τ, the amplitude of the first sum drops by a half when $\delta/T_2 \to 0.2$, and reaches its maximum when $\delta/T_2 \to 0$, $c_2(\delta) = 1$ and $c_4(\delta) = -1$ (see Fig. 4a and b), i.e., when the flippings of $M_\pm$ to $M_\mp$ and M_z to $-M_z$ are complete. Finally it should be noted that when the flippings are complete, the first sum can be reduced to the regular iDQC

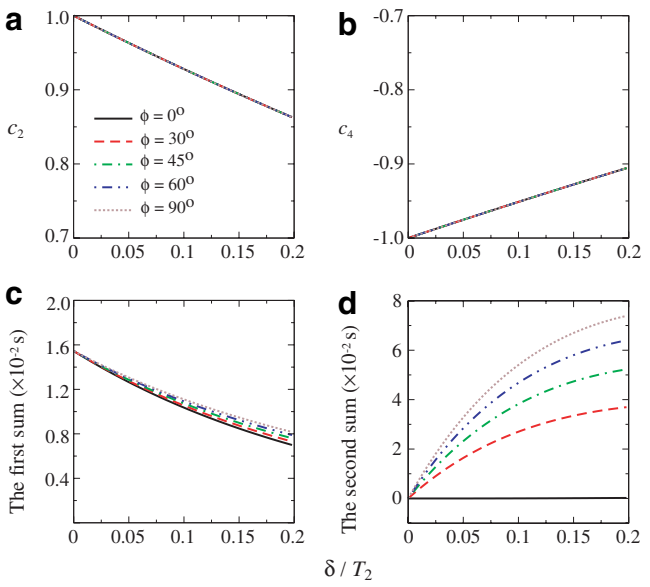

Fig. 4. The plot of (a) $c_2(\delta)$, (b) $c_4(\delta)$, (c) the magnitude of the first sum in Eq. (22a), and (d) the magnitude of the second sum in Eq. (22a) as a function of δ/T_2. Note that τ is fixed in the above plots. Therefore, the two sums in plots (c) and (d) show the implicit dependence on the incomplete flipping of $\vec{M}$ due to the T_2 decay. Parameters used are $n = 4$, $\phi_1 = 0$, $\tau_2 = 6$ ms, $t = \tau/2$, and $\tau = 2.7$ ms.

signal expression when the effect of finite pulse duration is ignored [27]:

$$M_+ \sim -\frac{e^{i\phi} m_1 \omega_d}{2} e^{(-1)^{n+1} i(\phi - 2\phi_1)} \{\tau_2 + t_T\} e^{-\frac{t_T}{T_2}}, \quad (25)$$

where $t_T = (n - \frac{1}{2})\tau + t$ is the total free evolution time in the multiple spin-echo sequence.

5.2. Rephasing of $M_\pm$ that happened during the refocusing pulses

Beside the rephasing of $M_\pm$ between the refocusing pulses in the multiple spin-echo sequence, $M_\pm$ is also rephased by the dipolar field during the pulses. This is represented by the second sum of Eq. (22a). In this case, $M_\pm$ undergoes dipolar field interaction ($K_{m\pm}(\delta)$) during one pulse, and interacts $(n-1)$ times with the rest of the pulses through either $c_1(\delta)$ or $c_2(\delta)$. Similar to the rephasing of $M_\pm$ at the time between the π pulses, the order k in $c_4(\delta)^k$ records the flipping history of M_z. Hence the term with factor $c_4(\delta)^k$ indicates the rephasing of $M_\pm$ that happened during the $(k+1)$th pulse. It should be noted that when $\delta \to 0$, the second sum of Eq. (22a) is zero and there is no rephasing of the iDQC signal that happened during the rf pulse.

Unlike the first sum of Eq. (22a), the amplitude of the second sum increases significantly when the flipping of $M_\pm$ is incomplete (Fig. 4d). Moreover, because of the factor $K_{m\pm}(\delta)$ in the second sum, the rephasing effect that happened during the π pulses is much more sensitive to the pulse phase difference $(\phi - 2\phi_1)$ than the rephasing effect that happened between the pulses (Fig. 4c). From Eq. (24), if $\phi = 2\phi_1 + m\pi$ with $m = 0, \pm 1, \pm 2, \ldots$, the factor $K_{m\pm}$ vanishes (to the first order of δ/T_2), and the rephasing effect that happened during the pulse is canceled. In contrast if $\phi = 2\phi_1 + (m + \frac{1}{2})\pi$, $K_{m\pm}$ attains its full magnitude, and the rephasing effect becomes maximal.

In Fig. 5, we calculate the signal for water and muscle with the phase difference $\phi - 2\phi_1 = 90°$. The dotted lines illustrate the situation when the dipolar field during the pulses is excluded ($d_i(t) = 0$, $i = 1, \ldots, 8$). Note that the signals in the free evolution periods (the unshaded regions in the figure) with and without considering the dipolar field during the pulses of finite duration depart from each other, which is in contrast to the coincidence of signals using $\phi - 2\phi_1 = 0$ in Fig. 2. This implies the rephasing of $M_\pm$ by the dipolar field that happened during a finite pulse is observable when $\phi - 2\phi_1 \neq m\pi$, where m is any integer. Moreover, we can see that the longer the rf pulses, the stronger the influence is the dipolar field on the signal.

The normalized transverse magnetizations ($|M_+|/M_0$) for water with $\phi_1 = 0$, different phases ϕ and pulse duration ratios r are plotted in Fig. 6. We can see from the figure that when the rephasing effect by the dipolar field during the rf pulses is not canceled ($\phi \neq 0$), the signals drop

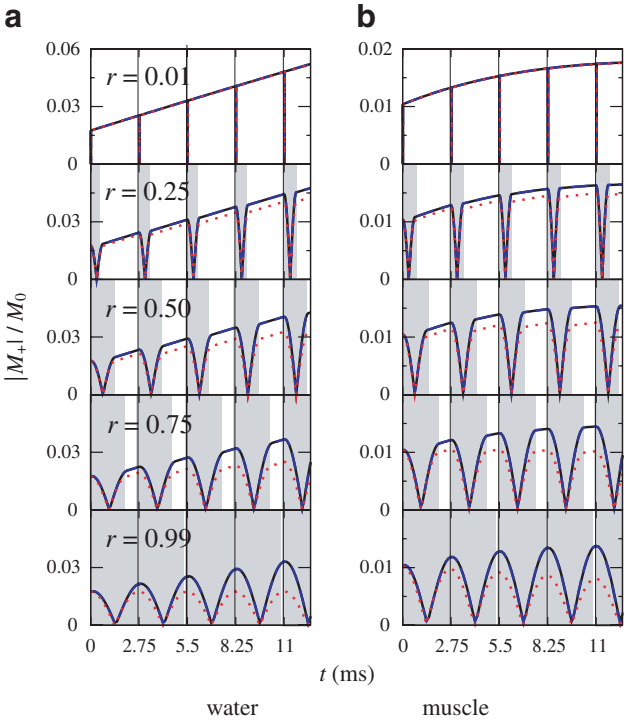

Fig. 5. The calculated magnitude of the normalized spatially averaged transverse magnetization against time using $\phi = 90°$ for (a) water and (b) muscle. The solid lines show the evolution of $|M_+|$ with both the transverse relaxation and the dipolar field effect taken account during the rf pulse, the dotted lines show the evolution of $|M_+|$ with the dipolar field effect during the pulses excluded, and the dashed lines (overlapped with the solid lines) show the linear approximation given by Eqs. (22) and (23). The grey regions depict the moment when the π pulses are applied, and the remaining regions represent the free evolution period. The parameters used in the calculations are $\tau_1 = 1.5$ ms, $\tau_2 = 6$ ms, $\phi_1 = 0°$, and $\tau + \delta = 2.75$ ms.

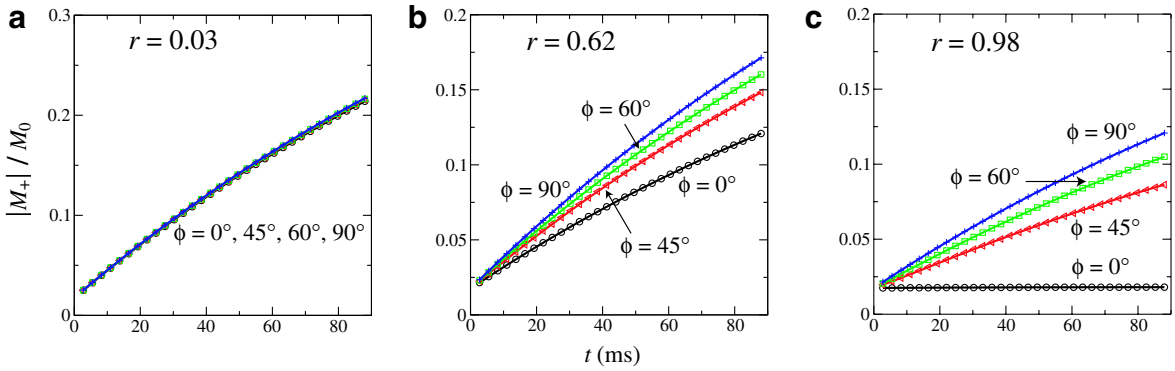

Fig. 6. The calculated signal for water with $\phi_1 = 0$, different phases ϕ and pulse duration ratios r: (a) $r = 0.03$, (b) $r = 0.62$, and (c) $r = 0.98$. We have used $\tau_1 = 1.5$ ms, $\tau_2 = 6$ ms, and $\tau + \delta = 2.75$ ms in the calculations.

less as r increases than the case when the rephasing effect during the rf pulses is canceled ($\phi = 0$).

6. Signal acquired in the multiple echo sequence

In the experiment of Ref. [28], a multiple spin echo acquisition was used to detect the iDQC signal of water. The phase of the first rf pulse in the CRAZED sequence is taken as $\phi_1 = 0$, and the phase of the refocusing pulses in the multiple spin-echo sequence is taken as $\phi = (0, 180°)$ for alternate pulses to compensate for imperfections. The experimental results are plotted in Fig. 7 with a comparison to the theoretical calculations without taking the long T_2 approximation. Small deviations from linearity are observed in experiment for long refocusing pulses and large number of pulses. This is due to small phase shifts caused by the hardware when switching between high amplitude and low amplitude pulses. The phase shift is measured to be about 16°. From the discussions of Section 5, this deviation from linearity originates from the rephasing of $M_\pm$ by the dipolar field that happened during the refocusing pulses. In Fig. 7, the theoretical calculations are plotted with the effects of phase shift and pulse imperfection taken into account. The calculated results are in good agreement with the experiment.

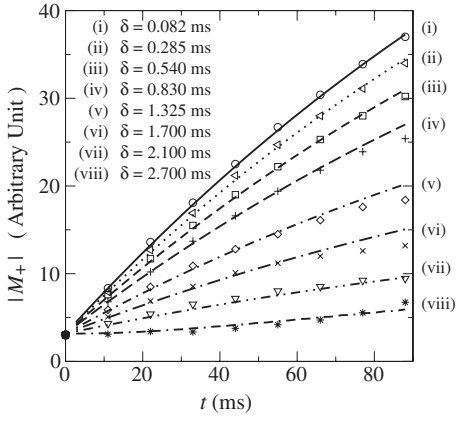

Fig. 7. The measured water signal (symbols) plotted against time with the calculated signal (smooth curves). We have used in the calculations $\phi_1 = 0°$, $\tau_1 = 1.5$ ms, $\tau_2 = 6$ ms, pulse separation $\tau + \delta = 2.75$ ms, flip angle of the refocusing pulses = 171° to simulate imperfect pulses with 5% error in the flipping angle, $\phi = (16°, 196°)$ for alternate refocusing pulses with pulse duration $\delta = 2.7$ ms, and $\phi = (0°, 180°)$ for alternate pulses with other pulse durations. A scaling factor is used in the calculated signals in order to compare the theory with the experiment. It is obtained by matching the measured signal with the theoretical calculations when very short pulse duration (82 μs in this case) is used.

The signal for instantaneous rf pulses (line (i)) rises with time in accordance with the regular iDQC signal expression given by Eq. (25). The finite rf pulses only delay and shorten the rise of the signal, as illustrated by Fig. 2. For sample like water with very long T_2, the condition $n\delta \ll T_2$ is satisfied even for the multiple echo acquisition with 32 pulses. Then with $\phi = \phi_1 = 0$, the signal in Eq. (22a) can be simplified as (see Appendix C)

$$M_{+,n} \simeq -\frac{1}{2} m_1 \omega_d (\tau_2 + n\tau)\, e^{-\frac{n\tau}{T_2}} \left(1 - \frac{n\delta}{T_2}\right). \tag{26}$$

It explains the observations in Fig. 3 and in [28] that the signal amplitude drops as a linear function of $n\delta/T_2$ when $n\delta \ll T_2$.

The monotonic increase in the signal in Fig. 7 is due to the dominant effect of the dipolar field when the T_2 of water is long. For muscle, T_2 is much shorter. When δ gets longer, the rising feature of the iDQC signal diminishes, and the signal is dominated by T_2 decay. In the case when δ occupies almost the whole multiple spin-echo sequence, i.e., $\tau \approx 0$, Eq. (23a) gives $F_1(n, m) = C_m^n \tau_2$. Then with $\phi = \phi_1 = 0$, Eq. (22a) reduces to

$$M_{\pm,n} = -\frac{1}{2} m_1 \omega_d \tau_2 \exp\left(-\frac{n\delta}{T_2}\right). \tag{27}$$

It describes the exponential decay $\exp(-n\delta/T_2)$ of the signal with very short τ as noted in Fig. 2 in Section 4.

7. Optimization of total acquired signal

In a multiple spin-echo sequence with N_π refocusing π pulses, the total acquired signal is proportional to S, which is defined by the normalized sum of the magnetizations as

Table 2
The optimal number of π pulses (N_π) and the corresponding free evolution period ($\tau = T/N_\pi - \delta$) that give the largest signal sum from a sequence of total time $T = 40$ ms and pulse durations $\delta = 1$ and 2 ms

Sample	Optimal N_π		Optimal τ (ms)	
	$\delta = 1$ ms	$\delta = 2$ ms	$\delta = 1$ ms	$\delta = 2$ ms
Water	21	10	0.9	2
Brain white matter	21	10	0.9	2
Muscle	21	11	0.9	1.6

The parameters used in the calculations are $\tau_1 = 1.5$ ms, $\tau_2 = 1$ ms, and $\phi_1 = \phi = 0$.

$$S = \sum_{n=1}^{N_\pi} |M_{+,n}|/M_0, \tag{28}$$

where $M_{+,n}$ is the spatially averaged magnetization at time $t = \frac{\tau}{2}$ after the nth refocusing pulse. In this way, the signal-to-noise ratio (SNR) can be raised by acquiring more echoes in a given period of time. However, in reality the number of acquired echoes is limited by the finiteness of the pulses.

As we have shown in Section 5, the iDQC signal rises primarily during the free evolution time between the refocusing pulses when the dipolar field effect during the refocusing pulses is canceled (see Fig. 2). This implies that when more π pulses are implemented in a given period of time, although the number of signal acquisition increases, the acquired signal is smaller because of the decrease in the free evolution period. We expect therefore the existence of an optimal number of pulses with the balance between the number of signal acquisitions and the length of the free evolution period that leads to the highest SNR.

We have calculated the total normalized signal S as a function of the number of acquired echoes N_π in a fixed period of time using parameters for water, muscle [33] and brain white matter [34]. With the multiecho acquisition time taken as $T = 40$ ms, T_2 of the three samples cover the ranges $T_2 > T$, $T_2 \sim T$ and $T_2 < T$. Table 2 summarizes the optimal number of π pulses and the corresponding free evolution period when the largest signal sum is obtained. It is interesting to note that even though the samples span a large range in T_2, the optimal signal in the three cases all take place when the pulse width δ is about half the pulse separation (T/N_π).

It is not clear currently why optimal signal occurs at $\delta \approx \tau$. Yet we expect that it can be generalized to other samples as it seems not to depend on T_2. A similar relation may exist for other iMQC signals, and possibly with different $\delta - \tau$ ratio.

8. Conclusions

We have studied the effect of the finite duration of refocusing pulses in a multiple spin-echo sequence on the signal formed under the influence of the dipolar field. Our results show that for the signal that is rephased by the dipolar field during the free evolution period, the finiteness of the pulses only delays and shortens the rise of the signal. As a result, signal is attenuated more in a pulse sequence with longer refocusing pulses. In addition, signal is also attenuated due to transverse relaxation during the pulses. The amount of signal drop reaches 50% when the ratio of the pulse duration to transverse relaxation (δ/T_2) goes up to 0.2.

We have obtained an analytic form of $\vec{M}$ for an arbitrary number of refocusing pulses in the long T_2 limit. The expressions show that the signal that is rephased between the π pulses is proportional to $(1 - n\delta/T_2)te^{-\frac{t}{T_2}}$. This explains the experimental observations that the signal rises linearly with the total free evolution time t and attenuates linearly with the total pulse duration $n\delta$. Moreover, the expressions suggest that there is a dependence on the phase of the refocusing pulses in the signal that is rephased by the dipolar field. The calculated signals are in good agreement with the experiment using water. It suggests that the first-order dipolar field approximation is sufficient in treating the problem when the coupling parameter is small, which is satisfied in most biological tissues.

Finally, we estimated the optimal pulse sequence parameters that can give the highest total acquired signal in the multiple spin-echo sequence of fixed duration and different pulse widths when the dipolar field effect is canceled during the refocusing pulses. We found that maximum SNR is obtained when the pulse duration is about half of the pulse separation for systems with a large range of T_2 values. It is clear from these results that with any multiecho implementation, such as a fast spin-echo (FSE), one must carefully balance the factors: the width of the π pulses, separation between and number of refocusing pulses, to minimize signal degradation.

Acknowledgments

Stimulating discussions with Dr. K.W. Chan and his help in proofreading this paper are gratefully acknowledged. This study is partially supported by a grant from the NIH (NS 41048).

Appendix A. The $d_i(t)$ coefficients

The coefficients $d_i(t)$, $i = 1, \ldots, 8$, in Eqs. (14) and (15) are found to be:

$$\begin{aligned} d_1(t) = & -\frac{ie^{-\frac{t}{T_2}}}{2a_0}\left\{\left(1-\frac{1}{a_0^2}\right)\sinh\frac{a_0 t}{T_2}\right. \\ & +\frac{(a_0-1)(a_0+3)}{2(a_0+1)}\sinh\frac{(a_0+1)t}{2T_2} \\ & \left.-\frac{(a_0+1)(a_0-3)}{2(a_0-1)}\sinh\frac{(a_0-1)t}{2T_2}+\frac{t}{a_0 T_2}\right\}, \end{aligned} \tag{A.1a}$$

$$d_2(t) = -\frac{\mathrm{i}\,\mathrm{e}^{-\frac{t}{T_2}}}{2a_0}\left\{-\left(1-\frac{1}{a_0^2}\right)\sinh\frac{a_0 t}{T_2} + \frac{(a_0-1)(a_0+3)}{2(a_0+1)}\sinh\frac{(a_0+1)t}{2T_2} - \frac{(a_0+1)(a_0-3)}{2(a_0-1)}\sinh\frac{(a_0-1)t}{2T_2} - \frac{t}{a_0 T_2}\right\}, \quad \text{(A.1b)}$$

$$d_3(t) = \frac{\gamma C T_2\,\mathrm{e}^{-\frac{t}{T_2}}}{4a_0^2}\left\{-\left(1-\frac{t}{T_2}\right) + \cosh\frac{a_0 t}{T_2} - \frac{1}{a_0}\sinh\frac{a_0 t}{T_2} - a_0\cosh\frac{(a_0-1)t}{2T_2} + \frac{2a_0}{a_0-1}\sinh\frac{(a_0-1)t}{2T_2} + a_0\cosh\frac{(a_0+1)t}{2T_2} - \frac{2a_0}{a_0+1}\sinh\frac{(a_0+1)t}{2T_2}\right\}, \quad \text{(A.1c)}$$

$$d_4(t) = \frac{\gamma C T_2\,\mathrm{e}^{-\frac{t}{T_2}}}{4a_0^2}\left\{-\left(1-\frac{t}{T_2}\right) + \cosh\frac{a_0 t}{T_2} - \frac{1}{a_0}\sinh\frac{a_0 t}{T_2} + a_0\cosh\frac{(a_0-1)t}{2T_2} - \frac{2a_0}{a_0-1}\sinh\frac{(a_0-1)t}{2T_2} - a_0\cosh\frac{(a_0+1)t}{2T_2} + \frac{2a_0}{a_0+1}\sinh\frac{(a_0+1)t}{2T_2}\right\}, \quad \text{(A.1d)}$$

$$d_5(t) = -\frac{\gamma C T_2\,\mathrm{e}^{-\frac{t}{T_2}}}{2a_0^2}\left\{-\left(1-\frac{t}{T_2}\right) + \cosh\frac{a_0 t}{T_2} - \frac{1}{a_0}\sinh\frac{a_0 t}{T_2}\right\}, \quad \text{(A.1e)}$$

$$d_6(t) = \frac{\gamma C T_2\,\mathrm{e}^{-\frac{t}{T_2}}}{a_0^2}\left\{-\left(1+\frac{t}{T_2}\right) + \cosh\frac{a_0 t}{T_2} + \frac{1}{a_0}\sinh\frac{a_0 t}{T_2}\right\}, \quad \text{(A.1f)}$$

$$d_7(t) = \frac{\gamma C T_2\,\mathrm{e}^{-\frac{t}{T_2}}}{2a_0}\left\{\cosh\frac{(a_0+1)t}{2T_2} + \frac{2}{a_0+1}\sinh\frac{(a_0+1)t}{2T_2} - \cosh\frac{(a_0-1)t}{2T_2} - \frac{2}{a_0-1}\sinh\frac{(a_0-1)t}{2T_2}\right\}, \quad \text{(A.1g)}$$

$$d_8(t) = -\frac{\mathrm{i}\,\mathrm{e}^{-\frac{t}{T_2}}}{8}\left\{\left[1-\frac{1}{a_0}\right]\sinh\frac{(a_0+1)t}{2T_2} - \left[1+\frac{1}{a_0}\right]\sinh\frac{(a_0-1)t}{2T_2}\right\}. \quad \text{(A.1h)}$$

Appendix B. The evaluation of $\{q\}$

The notation $\{q\}$ is defined as the set of permutation that records all the flipping orders of $M_\pm$ to $M_\mp$ after passing through n refocusing pulses. The symbol q_{nmjl} is the lth element of the jth permutation with m's flip and $(n-m)$'s unflip, where $q_{nmjl}=1$ when there is a flip of $M_\pm$ by the refocusing pulses associated with $c_2(\delta)$, and $q_{nmjl}=0$ when $M_\pm$ remains unchanged. Since there are C_m^n different ways to flip $M_\pm$ to $M_\mp$ by m out of n pulses, there are C_m^n different permuted sets in $\{q\}$.

As an example, for $(n,m)=(4,2)$, the first to the sixth ($C_m^n=6$) permuted sets of $\{q\}=\{\{1,1,0,0\},\{1,0,1,0\},\{1,0,0,1\},\{0,1,1,0\},\{0,1,0,1\},\{0,0,1,1\}\}$. Then the second element, for instance, of the third and the fifth permutated sets are $q_{4,2,3,2}=0$ and $q_{4,2,5,2}=1$.

Appendix C. The calculations of M_+ to the first order of δ/T_2

We have deliberately kept $c_1(\delta)$, $c_2(\delta)$, $c_4(\delta)$, $d_1(\delta)$, and $d_2(\delta)$ explicit in Eqs. (22) and (23). This enables us to evaluate the effects of different terms on the rephasing of $\vec{M}$ by the dipolar field at different time. By using Eqs. (12) and (16), we can further expand $M_\pm$ in Eq. (22a) to the first order of δ/T_2. With $\phi=\phi_1=0$,

$$\begin{aligned} M_{+,n}(t) &\simeq -\frac{m_1\omega_\mathrm{d}}{2}\,\mathrm{e}^{-\frac{t+(n-1/2)\tau}{T_2}} \times\left[c_1(\delta)^0 c_2(\delta)^n F_1(n,n) + c_1(\delta)^1 c_2(\delta)^{n-1} F_1(n,n-1)\right] \\ &\simeq -\frac{m_1\omega_\mathrm{d}}{2}\,\mathrm{e}^{-\frac{t+(n-1/2)\tau}{T_2}} \times\left[\left(1-\frac{3n\delta}{4T_2}\right)F_1(n,n) + \left(-\frac{\delta}{4T_2}\right)F_1(n,n-1)\right] \\ &\simeq -\frac{m_1\omega_\mathrm{d}}{2}\,\mathrm{e}^{-\frac{t+(n-1/2)\tau}{T_2}} \times\left[\tau_2+\left(n-\frac{1}{2}\right)\tau+t\right]\left(1-\frac{n\delta}{T_2}\right), \end{aligned} \quad \text{(C.1)}$$

where we have used

$$\begin{aligned} F_1(n,n) &= \tau_2+\frac{\tau}{2}+\left[\sum_{k=1}^{n-1}(-1)^{\sum_{l=1}^{k} q_{nm1l}} c_4(\delta)^k\right]\tau + (-1)^n c_4(\delta)^n t \simeq \tau_2+\frac{\tau}{2}+\left[\sum_{k=1}^{n-1}\left(1-\frac{k\delta}{2T_2}\right)\right]\tau \\ &\quad + \left(1-\frac{n\delta}{2T_2}\right)t = \left[\tau_2+\left(n-\frac{1}{2}\right)\tau+t\right] - \left[\frac{n(n-1)}{2}\tau+nt\right]\frac{\delta}{2T_2} \end{aligned} \quad \text{(C.2)}$$

and

$$\begin{aligned} F_1(n,n-1) &= \sum_{j=1}^{n}\left\{\tau_2+\frac{\tau}{2}+\left[\sum_{k=1}^{n-1}(-1)^{\sum_{l=1}^{k} q_{n,n-1,j,l}} c_4(\delta)^k\right]\tau + (-1)^{n-1} c_4(\delta)^n t\right\} \simeq \sum_{j=1}^{n}\left\{\tau_2+\frac{\tau}{2} + \left[\sum_{k=1}^{n-1}(-1)^{\sum_{l=1}^{k} q_{n,n-1,j,l}}(-1)^k\right]\tau + (-1)^{n-1}(-1)^n t\right\} = n\left(\tau_2+\frac{\tau}{2}-t\right). \end{aligned} \quad \text{(C.3)}$$

At $t=\tau/2$, we have

$$M_{+,n} \simeq -\frac{1}{2}m_1\omega_\mathrm{d}(\tau_2+n\tau)\,\mathrm{e}^{-\frac{n\tau}{T_2}}\left(1-\frac{n\delta}{T_2}\right). \quad \text{(C.4)}$$

References

[1] E. Hahn, Spin echoes, Phys. Rev. 80 (1950) 580–594.
[2] M. Bernier, J.M. Delrieu, Measurement of the susceptibility of solid ^{3}He along the melting curve from 20 mK down to the nuclear ordering temperature, Phys. Lett. A 60 (1977) 156–158.

[3] G. Deville, M. Bernier, J.M. Delrieux, NMR multiple echoes observed in solid ^{3}He, Phys. Rev. B 19 (1979) 5666–5688.
[4] W.S. Warren et al., Generation of impossible cross-peaks between bulk water and biomolecules in solution NMR, Science 262 (1993) 2005–2009.
[5] W. Richter et al., Imaging with intermolecular multiple-quantum coherences in solution nuclear magnetic resonance, Science 267 (1995) 654–657.
[6] J. Jeener, Equivalence between the "classical" and the "Warren" approaches for the effects of long range dipolar couplings in liquid nuclear magnetic resonance, J. Chem. Phys. 112 (2000) 5091–5094.
[7] R. Bowtell, P. Robyr, Structural investigations with the dipolar demagnetizing field in solution NMR, Phys. Rev. Lett. 76 (1996) 4971–4974.
[8] P. Robyr, R. Bowtell, Nuclear magnetic resonance microscopy in liquids using the dipolar field, J. Chem. Phys. 106 (1997) 467–476.
[9] P. Robyr, R. Bowtell, Measuring Patterson functions of inhomogeneous liquids using the nuclear dipolar field, J. Chem. Phys. 107 (1997) 702–706.
[10] R. Bowtell, S. Gutteridge, G. Ramanathan, Imaging long-range dipolar field in structured liquid samples, J. Magn. Reson. 150 (2001) 147–155.
[11] C. Ramanathan, R.W. Bowtell, NMR imaging and structure measurements using the long-range dipolar field in liquids, Phys. Rev. E 66 (2002) 041201.
[12] L.-S. Bouchard, R.R. Rizi, W.S. Warren, Magnetization structure contrast based on intermolecular multiple-quantum coherences, Magn. Reson. Med. 48 (2002) 973–979.
[13] L.-S. Bouchard, W.S. Warren, Reconstruction of porous material geometry by stochastic optimization based on bulk NMR measurements of the dipolar field, J. Magn. Reson. 170 (2004) 299–309.
[14] I. Ardelean, R. Kimmich, Diffusion measurements with pulsed gradient nonlinear spin echo method, J. Chem. Phys. 112 (2000) 5275–5280.
[15] S.M. Brown, P.N. Sen, D.G. Cory, Nuclear magnetic resonance scattering across interfaces via the dipolar demagnetizing field, J. Chem. Phys. 116 (2002) 295–301.
[16] S. Gutteridge, C. Ramanathan, R. Bowtell, Mapping the absolute value of M0 using dipolar field effects, Magn. Reson. Med. 47 (2002) 871–879.
[17] S.D. Kennedy, J. Zhong, Diffusion measurements free of motion artifacts using intermolecular dipole–dipole Interactions, Magn. Reson. Med. 52 (2004) 1–6.
[18] W.S. Warren, S. Ahn, M. Mescher, M. Garwood, K. Ugurbil, W. Richter, R.R. Rizi, J. Hopkins, J.S. Leigh, MR imaging contrast enhancement based on intermolecular zero quantum coherences, Science 281 (1998) 247–251.
[19] J. Zhong, Z. Chen, E. Kwok, New image contrast mechanisms in intermolecular double-quantum coherence human MR imaging, J. Magn. Reson. Imaging 12 (2000) 311–320.
[20] J. Zhong, Z. Chen, E. Kwok, In vivo intermolecular double-quantum imaging on a clinical 1.5 T MR scanner, Magn. Reson. Med. 43 (2000) 335–341.
[21] J. Zhong, E. Kwok, Z. Chen, fMRI of auditory stimulation with intermolecular double-quantum coherences (iDQCs) at 1.5 T, Magn. Reson. Med. 45 (2001) 356–364.
[22] W. Richter, M. Richter, W.S. Warren, H. Merkle, P. Andersen, G. Adriany, K. Ugurbil, Functional magnetic resonance imaging with intermolecular multiple-quantum coherences, Magn. Reson. Imaging 18 (2000) 489–494.
[23] R.R. Rizi, S. Ahn, D.C. Alsop, S. Garrett-Roe, M. Mescher, W. Richter, M.D. Schnall, J.S. Leigh, W.S. Warren, Intermolecular zero-quantum coherence imaging of the human brain, Magn. Reson. Med. 43 (2000) 627–632.
[24] S. Capuani, G. Hagberg, F. Fasano, I. Indovina, A. Castriota-Scanderbeg, B. Maraviglia, In vivo multiple spin echoes imaging of trabecular bone on a clinical 1.5 T MR scanner, Magn. Reson. Imaging 20 (2002) 623–629.
[25] X. Tang, H. Ong, K. Shannon, W.S. Warren, Simultaneous acquisition of multiple orders of intermolecular multiple-quantum coherence images, Magn. Reson. Imaging 21 (2003) 1141–1149.
[26] K.L. Shannon, R.T. Branca, G. Galiana, S. Cenzano, L.S. Bouchard, W. Soboyejo, W.S. Warren, Simultaneous acquisition of multiple orders of intermolecular multiple-quantum coherence images in vivo, Magn. Reson. Imaging 22 (2004) 1407–1412.
[27] J. Jeener, Collective effects in liquid NMR: dipolar field and radiation damping, in: D.M. Grant, R.K. Harris (Eds.), Supplement of the Encyclopedia of Nuclear Magnetic Resonance, Wiley, New York, 2002, pp. 642–679.
[28] S. Kennedy, Z. Chen, C.K. Wong, E.W.-C. Kwok, J. Zhong, Investigation of multiple-echo spin-echo signal acquisition under distant dipole–dipole interactions, Proc. Int. Soc. Magn. Reson. Med. 13 (2005) 2288.
[29] T. Enss, S. Ahn, W.S. Warren, Visualizing the dipolar field in solution NMR and MR imaging: three-dimensional structures simulations, Chem. Phys. Lett. 305 (1999) 101–108.
[30] M.P. Ledbetter, I.M. Savukov, L.-S. Bouchard, M.V. Romalis, Numerical and experimental studies of long-range magnetic dipolar interactions, J. Chem. Phys. 121 (2004) 1454–1465.
[31] C.P. Slichter, Principles of Magnetic Resonance, third ed., Springer-Verlag, Berlin, 1990.
[32] J.P. Marques, R. Bowtell, Optimizing the sequence parameters for double-quantum CRAZED, Imaging Magn. Reson. Med. 51 (2004) 148–157.
[33] C.K. Wong, T. Fallesen, P.R. Connelly, J. Zhong, Enhanced contrast of signal from distant dipolar field on relaxation times and B_0 in tissues, Proc. Int. Soc. Magn. Reson. Med. 11 (2004) 183.
[34] S.-P. Lee, A.C. Silva, K. Ugurbil, S.-G. Kim, Diffusion-weighted spin-echo fMRI at 9.4 T: microvascular/tissue contribution to BOLD signal changes, Magn. Reson. Med. 42 (1999) 919–928.